A Method for Extracting Airway Trees by Using a Cavity Enhancement Filter

Yasushi Hirano [1] *, Rui Xu [1], Rie Tachibana [2], and Shoji Kido [1]

[1] Applied Medical Engineering Science, Graduate School of Medicine, Yamaguchi University, Ube, Japan
yhirano@yamaguchi-u.ac.jp
[2] Information Science and Technology Dept., Oshima National College of Maritime Technology, Suou Oshima, Japan

Abstract. In this paper, a cavity enhancement filter and a novel method for extracting airway trees from three-dimensional (3D) CT images based on the cavity enhancement filter and the region-growing method are proposed. Since most previous methods for extracting airway trees reference bronchial branching information to track a bronchus, the tracking process could not accept abnormal bronchial branches, changes in the bronchus caused by pulmonary lobectomy, or a narrowed bronchus. The other type of methods for extraction is the region-growing based method. This method is robust over numerous variations of branching, but it is sensitive to the partial volume effect. The authors propose a novel method for extracting airway trees by using the region-growing method with the cavity enhancement filter that is also proposed by the authors. On the basis of the results of applying the proposed method to nine cases of 3D CT images, it was determined that the number and total length of the extracted bronchial branches increased while very few false positive regions were extracted.

1 Introduction

Extracting airway trees is important because these trees are useful for structural analyses of the lungs [1][2], virtualized bronchoscopy [3][4], and numerical simulations of respiratory functions [5]-[7]. For these purposes, a method for extracting precise airway trees is needed.

A number of methods have been proposed. They are categorized into three types:

Type I Simple region-growing based method that determines a single threshold of CT value over the whole image automatically [8][9]

Type II Tracking method that references information related to the bronchial branching structure [10]-[13]

* The authors would like thank Dr. Kazuhiro Ueda at Yamaguchi University, Japan for providing CT images. This research was supported by MEXT.KAKENHI (21103008), JSPS.KAKENHI (22300179).

Type III Voxel classification method [14]-[16]

Because methods belonging to Type I determine a single threshold of CT value, they would be easily affected by the partial volume effect (PVE). The PVE causes the stops of region growing and overflow. The methods in Type II are powerful because thresholds of CT value and parameters for enhancing bronchial walls can be determined for each bronchial branch, and exact bronchial structures are obtained during the tracking process. On the other hand, abnormal bronchial branching, changes in the bronchus caused by pulmonary lobectomy, or a tumor inside the bronchus would stop the tracking process. Type III is able to extract relatively precise airway trees by devising appropriate features and a classifier, but a large false positive (FP) might be extracted.

In this paper, the authors propose a novel method for preventing the effects of transformed airway trees and individual variations of branching patterns by combining Type I and III as well as a cavity enhancement filter (CEF).

2 Cavity enhancement filter

A bronchus is composed of an air region and a bronchial wall surrounding the air region. Hence, low CT values are distributed in the air region, and high CT values in the bronchial wall. The authors propose a "cavity enhancement filter", defined as the following equations for enhancing the air region in the bronchial wall.

$$g_{x,y,z} = \sum_{\substack{i,\,j,\,k\,\in\,\{-1,\,0,\,1\} \\ 9k+3j+i<0}} \max_{\substack{r_1=1,\ldots,R \\ r_2=1,\ldots,R}} \{L_{x,y,z}(i,j,k,r_1,r_2) - P_{x,y,z}(i,j,k,r_1,r_2)\} \quad (1)$$

$$L_{x,y,z}(i,j,k,r_1,r_2) = f_{x-ir_1,y-jr_1,z-kr_1} - 2f_{x,y,z} + f_{x+ir_2,y+jr_2,z+kr_2} \quad (2)$$

$$P_{x,y,z}(i,j,k,r_1,r_2) = |f_{x-ir_1,y-jr_1,z-kr_1} - f_{x+ir_2,y+jr_2,z+kr_2}|, \quad (3)$$

where $f_{x,y,z}$ and $g_{x,y,z}$ are the CT value and the output value of the CEF at voxel (x,y,z), respectively. Set $\{(x-i,y-j,z-k)|i,j,k \in \{-1,0,1\}, 9k+3j+i<0\}$ is half of the 26-neighborhood of voxel (x,y,z). Hence, Eq.(1) means a summation of the maximum values of a differences between $L_{x,y,z}$ and $P_{x,y,z}$ in each direction, and the maximum values are calculated in thirteen directions.

Here, $g_{x,y,z}$ takes a high value when the voxel (x,y,z) is in a cavity and a low value when no wall exists around the voxel (x,y,z). Furthermore, the CEF outputs high values at the air region inside the various radii of the bronchus wall by changing the radii of the filter. In Eq. (1) - (3), r_1 and r_2 represent the radii of the filter. This filter enhances cavities up to $2R$ in their diameters. $L_{x,y,z}$ looks like a second order differential, but it consists of two first order differentials with the same direction essentially. $P_{x,y,z}$ works as a penalty to inhibit the output of the CEF when a high CT region exists on only one side of voxel (x,y,z) in each direction. This means that voxel (x,y,z) is surrounded partially by a high CT region. Figure 1 shows an illustration of the CEF.

Figures 2 and 3 show the output of the CEF for artificial and CT images, respectively. It was determined that the CEF output high values on the voxels in the interior regions of tubes despite the radii of the tubes, the shapes of the tubes, or the addition of noise (Fig. 2). It was also determined that the CEF enhanced air regions inside of bronchi with various sizes of radii selectively (Fig. 3).

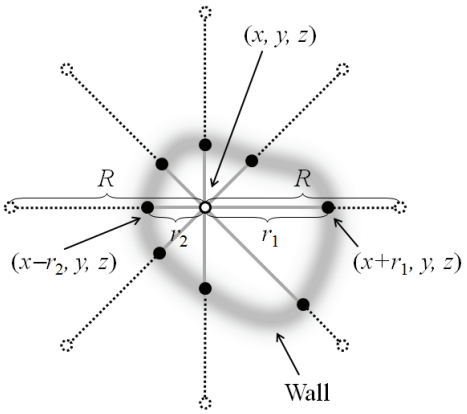

Fig. 1. Illustration of the CEF

3 Airway extraction method

3.1 Overview

First, the initial airway tree is extracted automatically using the region-growing based method [9]. The initial airway tree extracted by [9] contains very few FPs, and it can be used as a seed region in a precise extraction step for indicating the location of bronchi. Then, the candidate for the final airway tree is obtained by applying the region-growing method again. In the second application of the region-growing method, a combination of the difference in CT values and output of the CEF are used as a condition for extraction. Finally, small regions are deleted to reduce FPs.

Bronchi exist near the bronchial arteries. Therefore, the search region for the airway tree is limited to the neighborhood of the vessel region. Because of the difficulty in classifying bronchial arteries and bronchial veins, they are treated without classification in this paper. Figure 4 shows a flow chart of the proposed method.

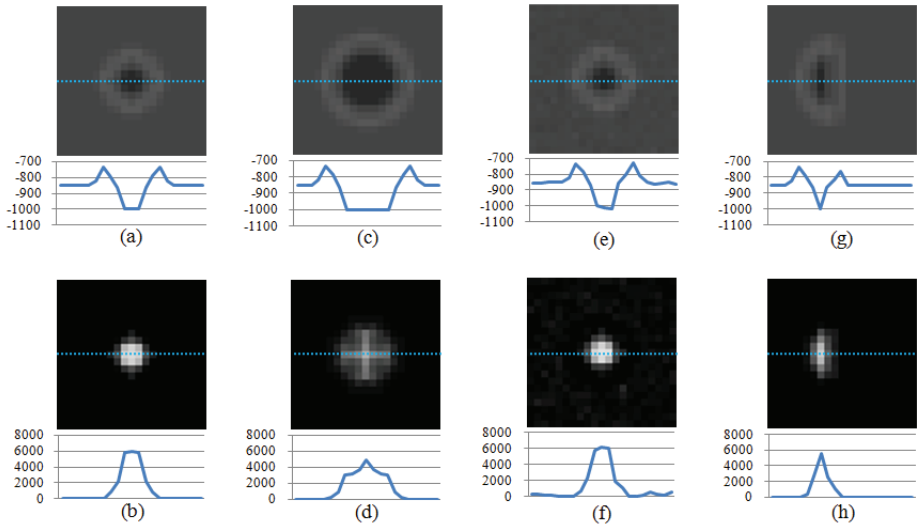

Fig. 2. Examples of output values of CEF (bottom) for artificial images (above). Figures under the images are profiles on the dotted lines represented by blue lines. All images are cross sections of 3D images. (a) is a tube with 4 voxels in the radius, (b) is the output for (a), (c) is a tube with 6 voxels in the radius, (d) is the output for (c), (e) is a tube with 4 voxels in the radius and Gaussian noise, (f) is the output for (e), (g) is a half tube with 4 voxels in the radius, and (h) is the output for (g).

3.2 Vessel-neighboring regions

As the authors mentioned above, the bronchi exist in the neighborhood of the blood vessels. The authors limited the region for searching airway trees to a neighborhood of blood vessels. This approach holds promise for reducing FPs.

First, the vessel regions are extracted using the method proposed in [17], which uses a method for enhancing line structures by using the Hessian matrix [18]. Then, the vessel regions are thinned using a thinning algorithm [19] and converted into a distance image by using a Euclidean distance transformation [20]. The distance image is multiplied by a constant value, and the thinning result is given by the distances on the corresponding voxel in the distance image. Finally, an inverse distance transformation is performed on the thinning result, and the vessel-neighboring region is obtained.

3.3 Region-growing

The proposed method uses the union of an initial airway tree obtained by the region-growing based method [9] and the region obtained by the CEF as seed regions for the second application of the region-growing method. The threshold for obtaining the seed regions is set to be sufficiently high so that the regions that are most likely to be the air region inside the bronchus are extracted. Then,

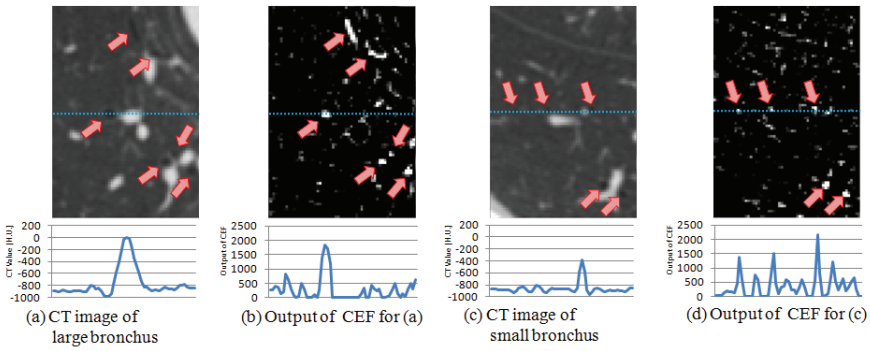

Fig. 3. Examples of output values of CEF [(b) and (d)] for CT images [(a) and (c)]. In the figures under the images, the profiles on the dotted lines are represented by the blue lines, and the red arrows indicate the locations of the bronchi.

the output value of the CEF and the CT value are used as conditions for region growing. Additionally, using multiple seed regions can avoid generating a large false negative (FN) in the distal portion of the airway trees. These FNs are most often caused by the PVE or tumors in the airway tree, and the methods in Type I and II often generate FNs.

The following two conditions are used for the second application of the region-growing method. When the current voxel of interest is voxel P, which is a candidate voxel of the airway tree region, and if the voxel Q in the 26-neighborhood of voxel P satisfies both the following two conditions, voxel Q is set to be a candidate of the airway tree region.

- Output value of CEF is higher than T_{CEF}.
- Difference in the CT values at voxels P and Q is less than T_{Diff}.

4 Experiments

4.1 CT images and parameter setting

The authors applied the proposed method to nine cases of 3D CT images. Specifications for the CT images were $512 \times 512 \times 347 - 517[voxels]$ for the image size, $0.625 - 0.762[mm]$ for the pixel spacing, and $1.0[mm]$ for the slice spacing. The parameters R in Section 2 and T_{CEF} and T_{Diff} in Section 3.3 were fixed for all cases and were 2, 2000, and 25, respectively. These parameters were determined in order to be obtained the best performance averagely.

4.2 Experimental results

Examples of the experimental results are shown in Fig. 5. The ground truth was determined manually by one of the authors at the advice of a medical doctor, and the previous method means the method proposed in [9].

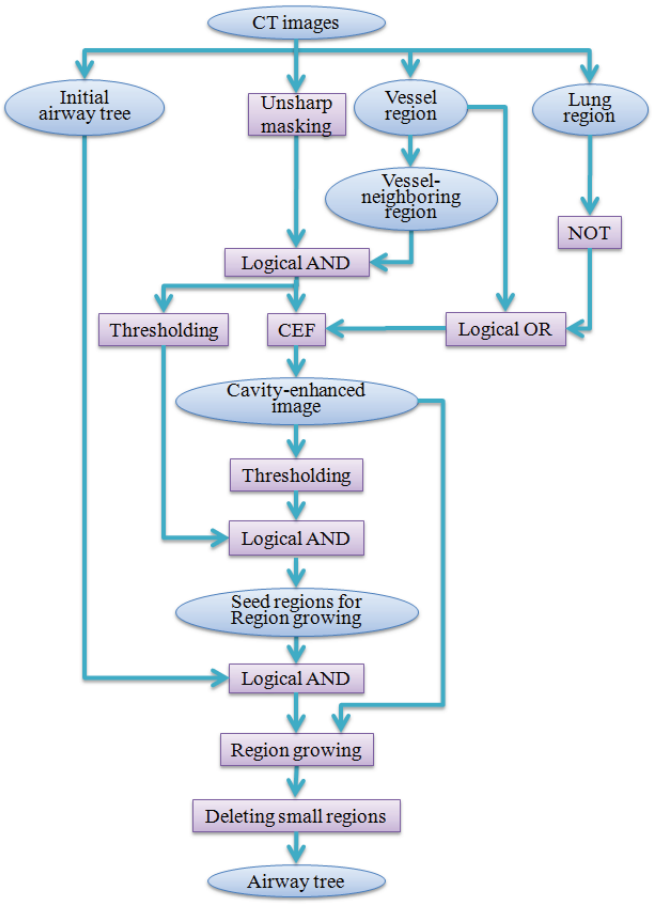

Fig. 4. Flow chart of the proposed method

The authors evaluated the experimental results by using the number of extracted branches, the ratio of extracted branches to the ground truth, the total length of the extracted branches, the ratio of the total length to the ground truth, and the FP ratio. The FP ratio is defined as the following equation, where "$\#A$" represents the number of voxels in region A.

$$FP\ ratio = \frac{\#(Extracted\ region \cap \overline{Ground\ truth})}{\#(Extracted\ region)} \tag{4}$$

A comparison of accuracy with the proposed method and with the previous method is shown in Table 1.

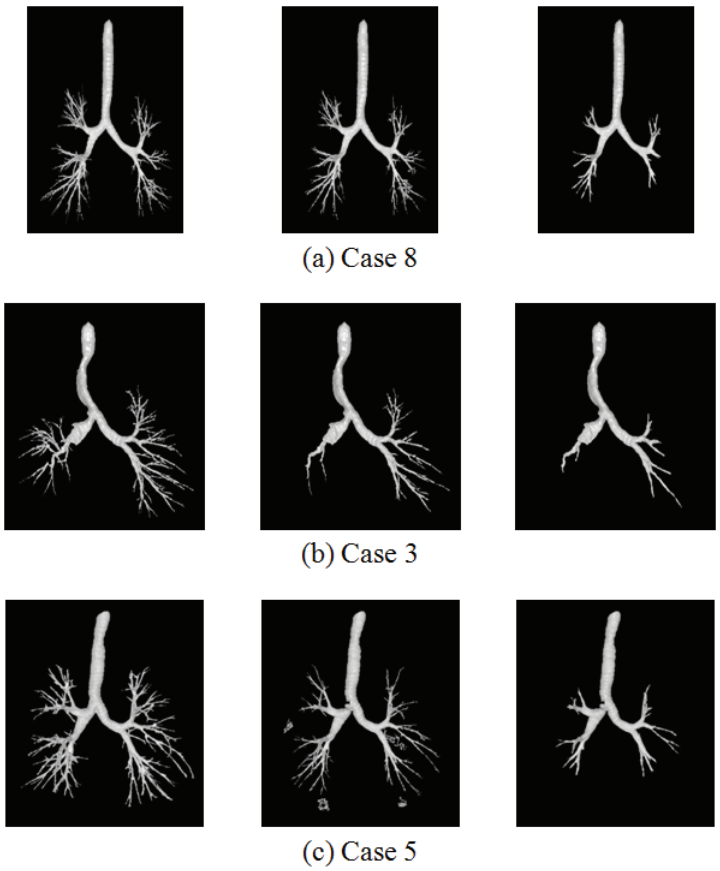

Fig. 5. Experimental results. The ground truth (left), the proposed method (middle), and the previous method (initial airway tree; right) for Case 8 (above), Case 3 (middle), and Case 5 (bottom), respectively.

5 Discussion

As shown in Table 1, the maximum, minimum, and average ratios of the number of extracted branches with the proposed method were 0.860, 0.391, and 0.558, respectively. The ratios with the previous method were 0.258, 0.106 and 0.177, respectively. The proposed method had about a three times better performance than the previous method. Especially, the ratio for Case 8 with the proposed method was 0.860, and almost all non-peripheral bronchi could be extracted successfully [Fig.5(a)]. While the proposed method had a good performance for almost all cases, the ratio of the extracted branches for Case 3 [Fig. 5(b)] was relatively low. A pulmonary lobectomy was performed for Case 3, and the right upper and middle lobes were removed. This surgical operation caused a large deformation and stenosis of the bronchi. Similarly, little or no thin bronchi with

Table 1. Comparison of results by the proposed method and the previous method [9].

		Case								
		1	2	3	4	5	6	7	8	9
Proposed method	Number of branches	613	187	207	151	373	149	441	555	359
	Ratio of extracted branches (Number)	0.496	0.426	0.447	0.549	0.523	0.391	0.607	0.860	0.722
	Total length (mm)	27830	11138	9908	7949	18956	9391	21725	19817	17483
	Ratio of extracted branches (Length)	0.556	0.523	0.471	0.499	0.557	0.437	0.540	0.775	0.771
	FP/(TP+FP)	0.003	0.007	0.000	0.008	0.029	0.004	0.007	0.004	0.004
Previous method	Number of branches	131	59	71	71	127	69	85	139	125
	Ratio of extracted branches (Number)	0.106	0.134	0.153	0.258	0.178	0.181	0.117	0.216	0.252
	Total length (mm)	8206	3797	4488	4651	7876	4449	4911	6983	7354
	Ratio of extracted branches (Length)	0.164	0.178	0.213	0.292	0.231	0.207	0.122	0.273	0.324
	FP/(TP+FP)	0.006	0.000	0.000	0.000	0.000	0.000	0.000	0.000	0.000
Ground truth	Number of branches	1235	439	463	275	713	381	727	645	497
	Total length (mm)	50028	21293	21025	15936	34034	21493	40216	25557	22687

1 or 2 voxels in their diameter were extracted for all cases even though the rate of the mis-extracted branches was low. This means that enhancing cavities by using the CEF is insufficient for thin airways.

FP ratios were very low for almost all cases except for Case 5 [Fig. 5(c)]. Case 5 had many low attenuation areas (LAAs) in the peripheral region of its lungs, and these LAAs caused a high FP ratio.

6 Summary

In this paper, a cavity enhancement filter for enhancing the air region inside the bronchial wall and a novel method for extracting airway trees from 3D CT images by using the region-growing based method with the CEF were proposed. The proposed method for extracting airways tree improved accuracy in comparison with the previous method [9]. The FP of the proposed method was much less than that of the previous similar methods [15] with almost the same extraction rate.

Future work includes the development of a more powerful enhancement method for cavities, an automatic and adaptive determination of thresholds, an improvement in the accuracy of extraction, and the reduction of FPs.

References

1. Zhou, X., Hayashi, H., Hara, T., Fujita,H., Yokoyama, R., Kiryu, T., Hoshi, H. : Automatic recognition of lung lobes and fissures from multi slice CT images. Proc. SPIE on Medical Imaging, pp.1629–1633, 5370 (2004)
2. Mekada, Y., Nakamura, S., Ide, I., Murase, H., Otsuji, H. : Pulmonary artery and vein classification using spatial arrangement features from X-ray CT images. Proc. the 7th Asia-pacific Conference on Control and Measurement (2006)

3. Mori, K., Ota, S., Deguchi, D., Kitasaka, T., Suenaga, Y., Iwano, S., Hasegawa, Y., Takabatake, H., Mori, M., Natori, H., : Automated Anatomical Labeling of Bronchial Branches Extracted from CT Datasets Based on Machine Learning and Combination Optimization and Its Application to Bronchoscope Guidance. Proc. Medical Image Computing and Computer-Assisted Intervention (MICCAI) 2009, Part II, LNCS 5762, pp.707–714 (2009)
4. http://www.gehealthcare.com/euen/ct/products/clinical_applications/products/virtualendoscopy.html
5. Lin, C.L., Hoffman, E.A. : A numerical study of gas transport in human lung models. Proc. SPIE on Medical Imaging, pp.92–100, 5746 (2005)
6. Hylla, E., Frederich, O., Thiele, F., Wang, X., Wegner, I., Meinzer, H.P., Puderbach, M. : Flow in naturally changing central airways. Proc. European Conference on Computational Fluid Dynamics (ECCOMAS CFD) 2010, (2010)
7. Hirano, Y., Xu, R., Kido, S., Chen, X., Ishii, K. : Numerical simulation of respiratory function for pulmonary lobectomy. Proc. International Forum on Medical Imaging in Asia (IFMIA) 2011, pp.111–112 (2011)
8. Mori, K., Hasegawa, J., Toriwaki, J., Anno, H., Katada, K. : Automated extraction and visualization of bronchus from 3D CT images of lung. Proc of 1st. CVRMed'95, pp.542–548 (1995)
9. Yamamura,H., Shouno,H., Kido, S. : Fully Automatic Segmentation of Pulmonary Lobes from Three dimensional Thoracic CT images. RSNA2007 (2007)
10. Kitasaka, T., Mori, K., Hasegawa, J., Toriwaki, J. : A Method for Extraction of Bronchus Regions from 3D Chest X-ray CT Images by Analyzing Structural Features of the Bronchus. Forma, Vol.17, pp.321–338 (2002)
11. Tschirren, J., Hoffman. E.A., McLennan, G., Sonka, M. : Airway tree segmentation using adaptive regions of interest. Proc. SPIE on Medical Imaging, 5369, 117 (2004)
12. Graham, M.W., Gibbs, J.D., Higgins, W.E. : Robust system for human airway-tree segmentation. Proc. SPIE on Medical Imaging, 6914, 69141J (2008)
13. Feuerstein, M., Kitasaka, T., Mori, K. : Adaptive Branch Tracing and Image Sharpening for Airway Tree Extraction in 3-D Chest CT. Proc. Second International Workshop on Pulmonary Image Analysis, pp.273–284 (2009)
14. Lo, P., Bruijne, M. : Voxel classification based airway tree segmentation. Proc. SPIE on Medical Imaging, 6914, 69141K (2008)
15. Kitasaka, T., Yano, H., Feuerstein, M., Mori, K. : Bronchial region extraction from 3D chest CT image by voxel classification based on local intensity structure. Proc. Third International Workshop on Pulmonary Image Analysis, pp.21–29 (2010)
16. Fetita, C.I., Preteux, F.J. : Bronchial tree modeling and 3D reconstruction. Proc. SPIE on Mathematical Modeling, Estimation, and Imaging, 4121, 16 (2000)
17. Shikata, H., Hoffman, E.A., Sonka, M. : Automated segmentation of pulmonary vascular tree from 3D CT images. Proc. SPIE on Medical Imaging, 5369, 107 (2004)
18. Sato, Y., Nakajima, S., Shiraga, N., Atsumi, H., Yoshida, S., Koller, T., Gerig, G., Kikinis, R. : Three-dimensional multi-scale line filter for segmentation and visualization of curvilinear structures in medical images. Medical Image Analysis, Vol.2, No.2, pp.143–168 (1998)
19. Saito, T., Toriwaki, J. : A sequential thinning algorithm for three dimensional digital pictures using the Euclidean distance transformation. Proc. 9th SCIA (Scandinavian Conf. on Image Analysis), pp.507–516 (1995)
20. Saito, T., Toriwaki. J. : New algorithms for n-dimensional Euclidean distance transformation. Pattern Recognition. Vol.27, No.11, pp.1551–1565 (1994)